Acta Cryst. (1968). B24, 637

A Structural Investigation of Some Stable Phases in the Region $Nb_2O_5.WO_3$–WO_3

BY N.C. STEPHENSON

School of Chemistry, University of New South Wales, Sydney, Australia

(*Received* 27 *May* 1967 *and in revised form* 29 *August* 1967)

A 'single' crystal of the compound $6Nb_2O_5.11WO_3$ has been shown to be an intergrowth of two stable phases; an orthorhombic $9Nb_2O_5.16WO_3$ and a monoclinic $9Nb_2O_5.17WO_3$ which is also twinned on the (100) plane. The structures are based upon a tetragonal-bronze subcell, a two-dimensional network of corner-sharing octahedra which extend in a third direction, again by corner sharing. This host structure extends through the matrix of intergrowing phases and the differing unit cells and symmetries arise from the manner in which the five-membered rings, which become tunnels in three dimensions, are filled with metal and oxygen atoms. The metal atoms in these tunnels have sevenfold coordination. A comparison of the structures of the compounds $9Nb_2O_5.16WO_3$, $4Nb_2O_5.9WO_3$ and $9Nb_2O_5.17WO_3$ shows that the pentagonal tunnels are filled according to a close packed hexagonal or cubic array. It is possible, using these building principles, to predict the structure of the compound $2Nb_2O_5.7WO_3$.

Many stable phases exist in the binary system Nb_2O_5–WO_3. The region Nb_2O_5–$Nb_2O_5.WO_3$ has been recently subjected to intensive investigation. On the basis of single-crystal X-ray diffraction studies, Roth & Wadsley (1965) reported the existence of five compounds occurring at $Nb_2O_5.WO_3$ ratios of 15:1, 6:1, 7:3, 8:5 and 9:8. These compounds are structurally related to Nb_2O_5 (Gatehouse & Wadsley, 1964) in that each one contains ReO_3-type octahedral blocks joined to similar blocks at different levels along a short axis (3·9 Å) by edge sharing. There are tetrahedrally coordinated W atoms ordered at the junctions of every four blocks. The 'building block' principle was elaborated as the basis of the crystal chemistry of the niobate compounds and a large number of compounds are foreseen with structures resembling the above members but containing wider blocks instead, *e.g.* $5\times n\times\infty$. Such compounds, which might be induced to form under the proper experimental conditions, have not yet been discovered or characterized although Roth & Waring (1966) have recently reported a 30:1 phase and Andersson, Mumme & Wadsley (1966) have reported the structure of $13Nb_2O_5.4WO_3$ as consisting of a mixture of blocks of $3\times4\times\infty$ and $4\times4\times\infty$, occurring in alternate sequence to make an ordered intergrowth structure.

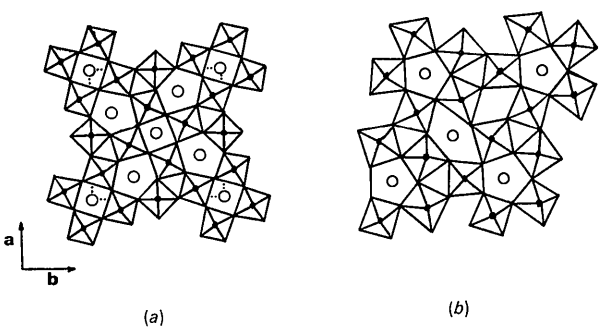

Fig. 1. (*a*) The tetragonal bronze structure, $Ba_6Ti_2Nb_8O_{30}$, viewed in projection along [001]. The five-membered rings are filled with metal atoms only. (*b*) The structure of $NaNb_6O_{15}F$ viewed in projection. The five-membered rings are filled with metal atoms and oxygen atoms, giving rise to pentagonal bipyramidal coordination.

The above series of Nb/W oxides which are structurally related to Nb_2O_5 and which can be described by the homologous series notation $B_{nmp+1}O_{3nmp-(n+m)p+4}$ does, for reasons still not clearly understood, stop at the phase $W_8Nb_{18}O_{69}$. The next sequence of phases, richer in WO_3 and commencing at $Nb_2O_5.WO_3$, probably contains members of a new series of structurally related stoichiometric compounds, but with a building principle of a different kind. It is about these compounds that this paper is concerned.

Previous work

In the region $Nb_2O_5.WO_3$–WO_3 the following compounds have been established as discrete phases by using single-crystal data and phase equilibria studies:

(*a*) $Nb_2O_5.WO_3$ (WNb_2O_8)

First reported by Fiegel, Mohanty & Healy (1964) and confirmed by Roth & Wadsley (1965). Single-crystal precession photographs (Roth & Waring, 1966) enabled the cell dimensions and space group listed in Table 1 to be deduced. WNb_2O_8 is believed to be structurally related to WTa_2O_8 (Andersson & Lundberg, 1966) which contains octahedrally coordinated cations sharing corners to form rings of five octahedra such as exist in the tetragonal potassium tungsten bronze (K_xWO_3) structure (Magnéli, 1949). Within each ring is a cation in sevenfold coordination together with an additional oxygen atom, in a pentagonal-bipyramidal configuration.

(*b*) $4Nb_2O_5.9WO_3$ ($Nb_8W_9O_{47}$)

First reported by Roth & Wadsley (1965). This compound was examined by Sleight & Magnéli (1964) and the structure reported in some detail by Sleight (1966). The crystal structure was found to be made up of three tetragonal-bronze-like unit cells with four out of the twelve possible fivefold rings occupied by cations with oxygen atoms above and below, forming pentagonal bipyramid coordination polyhedra.

(*c*) $2Nb_2O_5.7WO_3$ ($Nb_4W_7O_{31}$)

First reported by Roth & Wadsley (1965). The unit-cell dimensions listed in Table 1 were obtained from X-ray diffraction powder data listed by Roth & Waring (1966).

(*d*) $6Nb_2O_5.11WO_3$ ($Nb_{12}W_{11}O_{63}$)

The phase to which Kovba & Trunov (1964) assigned the composition $4Nb_2O_5.7WO_3$ and which Roth & Wadsley (1965) reported to be $13Nb_2O_5.24WO_3$ is the compound $6Nb_2O_5.11WO_3$ described by Roth & Waring (1966). The unit-cell dimensions, obtained from powder data, indicate that the structure is again related to the tetragonal potassium tungsten bronze.

(*e*) $3Nb_2O_5.8WO_3$ ($Nb_6W_8O_{39}$)

Goldschmidt (1960), Kovba & Trunov (1962) and Fiegel, Mohanty & Healy (1964) each reported a phase at about the composition $Nb_2O_5.3WO_3$. In their extensive phase equilibria studies on the Nb/W oxide system Roth & Waring (1966) regard this phase as metastable and based upon a disordered tetragonal bronze-type phase with no indication of superstructure. The composition is 3:8.

Present work

The tetragonal tungsten bronze structure [Fig. 1(*a*)] was deduced by Magnéli (1949) for the phase K_xWO_3 ($0{\cdot}48 < x < 0{\cdot}54$). It can be viewed as a two-dimensional network of corner-sharing octahedra which extends in a third direction again by corner sharing. These networks form 3-, 4- and 5-membered rings which become tunnels in three dimensions. Six-sided tunnels occur in compounds such as $MoW_{3n-1}O_{9n}$ ($n=4,5$) (Graham & Wadsley, 1961). The tunnels may be empty as in the above $MoW_{11}O_{36}$ and in ReO_3; they may be partially filled as in the various tungsten bronzes of the type A_xWO_3 (Hägg & Magnéli, 1954) or they may be fully filled with cations as in $Ba_6Ti_2Nb_8O_{30}$ (Stephenson, 1965). In this latter instance the barium ions occupying the five-sided tunnels have tenfold coordination with oxygen atoms since the barium ions do not lie in the same plane as the octahedrally coordinated metal atoms.

The five-sided tunnels may also be filled with metals and oxygen atoms to form a string of pentagonal bipyramids which share apices. In this case all metal atoms lie in the same plane. Such examples are $Mo_{17}O_{47}$ (Kihlborg, 1963), $NaNb_6O_{15}F$ and $NaNb_6O_{15}OH$ [Fig. 1(*b*)] (Andersson, 1965). The Nb/W oxides occurring as single phases within the region $Nb_2O_5.WO_3$–WO_3 of the phase diagram, and listed in Table 1, are believed to have superstructures based upon the tetragonal tungsten-bronze in which some of the pentagonal tunnels are occupied by metal and oxygen atoms. The structures of the 6:11, 4:9 and 2:7 phases are reported below and confirm this belief.

An investigation of the crystal structure of $6Nb_2O_5.11WO_3$

The compound $Nb_{12}W_{11}O_{63}$ is stable from about 1210 °C to 1378 °C, when it melts congruently. Crystals were prepared by Dr R. S. Roth at the National Bureau of Standards, Washington, D.C., U.S.A. Stoichiometric amounts of Nb_2O_5 and WO_3 were heated in a sealed platinum tube for 68 hours at 1355 °C and then quench cooled. The results of the crystal structure analysis have shown that the composition of this metastable phase at room temperature is $Nb_{12}W_{11}O_{63}$ and there is no reason to suppose it differs from the stable, high temperature preparation.

Experimental

X-ray data were collected from a small needle shaped crystal, 0·02 cm in length and average cross sectional diameter of 0·005 cm. Zero layer precession photographs taken with Mo $K\alpha$ radiation yielded cell dimensions in excellent agreement with those listed by Roth & Waring (1966) *i.e.* $a=12{\cdot}195$, $b=36{\cdot}740$, $c=3{\cdot}951$ Å. The c axis of the orthorhombic cell is parallel to the needle axis of the crystal. The only systematic absences noted in diffraction data occurred for reflexions $h00$ with $h=2n+1$ and $0k0$ with $k=2n+1$. The space group was therefore taken to be $P2_12_12$.

Equi-inclination Weissenberg geometry, with Cu $K\alpha$ radiation, was used to collect $hk0$-3 data and intensities were estimated visually with the use of multiple film techniques and a standard series of spots recorded in the usual manner. The intensity reduction programs

Table 1. *Crystallographic data for some discrete phases existing in the region* $Nb_2O_5.WO_3$–WO_3

Mole ratio Nb_2O_5	Mole ratio WO_3	Symmetry	Possible space groups	Unit-cell dimensions (Å) a	b	c
1	1	Orthorhombic	*Pmab*, $P2_1ab$	16·615	17·616	3·955
4	9	Orthorhombic	$P2_12_12$	36·692	12·191	3·945
2	7	Tetragonal		24·264		3·924
6	11	Orthorhombic	$P2_12_12$	12·195	36·740	3·951
3	8	Tetragonal		12·190		3·968

of Sime (1961) for use with the UTECOM digital computer were used for the Weissenberg data.

Atomic form factors for oxygen and for niobium and tungsten were taken from Hoerni & Ibers (1954) and from Thomas & Umeda (1957) respectively. The zero oxidation state was taken for each element owing to an uncertainty in the relative degrees of ionicity, and the correctness of this assumption was expected to be reflected in the temperature factors of the various atoms. Corrections for the real component of the anomalous dispersion of Cu $K\alpha$ by tungsten and niobium were made with the $\Delta f'$ values given by Dauben & Templeton (1955). Most of the calculations involved in the crystal structure analysis were facilitated by the use of the UTECOM and IBM 7040 digital computers.

Structure determination

A survey of the corrected intensities drew attention to a nearly identical distribution for zero and upper level reflexions. Also, *hkl* data were particularly intense for $k=3n$, and it seems that the structure is based upon the tetragonal bronze subcell, tripled along the **b** direction, with all atoms lying close to the (001) and (002) planes and with metal atoms in one of these planes. The (001) Patterson projections for the tetragonal bronze $Ba_6Ti_2Nb_8O_{30}$ and for $Nb_{12}W_{11}O_{63}$ are shown in Fig. 2 for comparison.

In view of the short length of the *c* axis, an endeavour was made to solve the structure in projection, using *hk*0 data only. Multiple minimum function methods applied to the (001) Patterson projection quickly yielded the coordinates of metal atoms in octahedral environment and these were refined by successive cycles of structure factors (F_{metals}) and ($F_o - F_{\text{metals}}$) difference Fourier syntheses. Equal peak heights indicated a statistical distribution of niobium and tungsten atoms over these sites and an average form factor, 12Nb+11W/23, was used, based upon the relative numbers of metal atoms in the unit cell.

During the above course of refinement cycles the oxygen atoms which did not project on metal atoms, *i.e.* those in the same plane as the metal atoms were located and led to the host lattice, or complex of corner-sharing octahedra depicted in Fig. 3. This two-dimensional network extends in a third direction, along the axis of projection, again by corner-sharing. The twelve pentagonal rings *each* appeared to be occupied but with varying degrees of occupancy. Attempts to refine this model by full-matrix least-squares methods and by difference Fourier syntheses, were without success. In the former case the average form factor was used for metal atoms and occupancy factors for metal sites were allowed to vary so as to detect any tendency to order. The results indicated a statistical distribution of W

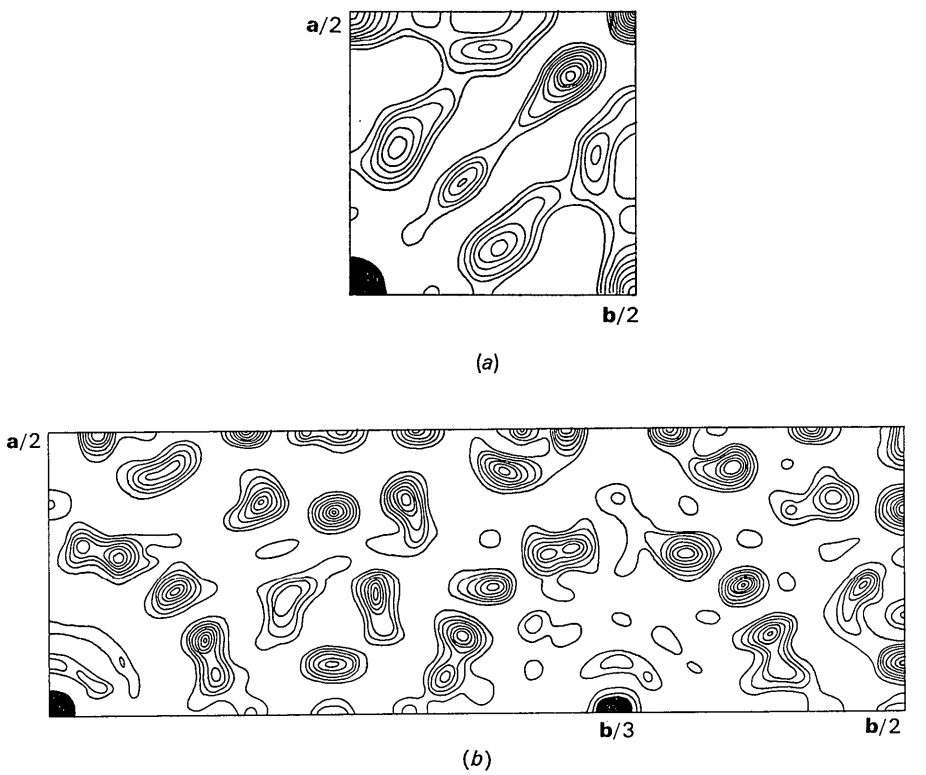

Fig. 2. (*a*) The (001) Patterson projection for the tetragonal bronze $Ba_6Ti_2Nb_8O_{30}$. (*b*) The (001) Patterson projection for the compound $Nb_{12}W_{11}O_{63}$, drawn to the same scale as (*a*).

and Nb atoms over the octahedral sites, as evidenced by equal occupancy factors, but the identification of atoms in the pentagonal tunnels and the mechanism by which these tunnels were filled was difficult to comprehend.

Identification of intergrowth phases

The full use of three-dimensional data was now considered essential for the structure determination of $Nb_{12}W_{11}O_{63}$. It was during the investigation of upper level Weissenberg data that what was originally thought to be a gradual spot broadening was in fact found to be due to spot splitting. The *hk*2 and *hk*3 data, under magnification, each split into three. Spot splittings occur perpendicular to the Weissenberg festoons which have a constant *h* index [Fig. 4(*a*)] and a diagrammatic representation of this phenomenon is shown in Fig. 4(*b*).

The 'single' crystal of $Nb_{12}W_{11}O_{63}$ is an intergrowth of two phases, one having an orthorhombic and the other a monoclinic unit cell. The monoclinic phase is twinned on the (100) plane so that *hkl* and $\bar{h}kl$ reflexions from this system lie either side of a corresponding *hkl* reflexion from the orthorhombic crystal. In ac-

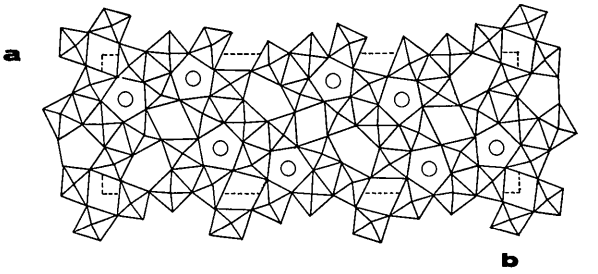

Fig. 3. The complex of corner-sharing octahedra which represents the host structure in the compound $Nb_{12}W_{11}O_{63}$. Projection along [001]. The circles represent metal and oxygen atoms (superimposed) which occupy pentagonal rings in the orthorhombic phase.

Table 2. *Atomic parameters for* $6Nb_2O_5.11WO_3$

Standard deviations are given in brackets and refer to the last two (or three) places of the preceding number.

Metal atoms*

	x/*a*	*y*/*b*	*z*/*c*	Occupancy (*p*)	Peak height
M(1)	0·50000	0·00000	0·00000	1·022 (70)	55·2 e.Å^{-3}
M(2)	0·20460 (98)	0·02843 (44)	0·00000	1·073 (56)	57·9
M(3)	0·42810 (105)	0·09827 (39)	0·00000	1·207 (60)	65·2
M(4)	0·00886 (101)	0·16258 (40)	0·00000	1·094 (62)	59·1
M(5)	0·28692 (110)	0·18906 (39)	0·00000	1·092 (58)	59·0
M(6)	0·06341 (109)	0·26450 (42)	0·00000	1·127 (58)	60·8
M(7)	0·20890 (105)	0·35742 (40)	0·00000	1·069 (59)	57·7
M(8)	0·41676 (110)	0·43456 (40)	0·00000	1·031 (57)	55·7
M(9)	0·17178 (333)	0·10070 (117)	0·00000	0·245 (47)	7·3
M(10)	0·34027 (140)	0·27952 (58)	0·00000	0·781 (42)	40·0
M(11)	0·17011 (194)	0·44394 (74)	0·00000	0·532 (44)	24·0

* M = 12Nb + 11W/23.

Oxygen atoms

	x/*a*	*y*/*b*	*z*/*c*
O(1)	0·4426	0·0428	0·0000
O(2)	0·0679	0·0581	0·0000
O(3)	0·2875	0·0667	0·0000
O(4)	0·3236	0·1426	0·0000
O(5)	0·1623	0·1797	0·0000
O(6)	0·1975	0·2296	0·0000
O(7)	0·0013	0·2075	0·0000
O(8)	0·1845	0·3072	0·0000
O(9)	0·0764	0·3914	0·0000
O(10)	0·3213	0·4045	0·0000
O(11)	0·3366	0·0054	0·0000
O(12)	0·3460	0·4790	0·0000
O(13)	0·3610	0·3230	0·0000
O(14)	0·4100	0·2265	0·0000
O(15)	0·0160	0·1335	0·0000
O(16)	0·5000	0·0000	0·5000
O(17)	0·2046	0·0284	0·5000
O(18)	0·4281	0·0983	0·5000
O(19)	0·0089	0·1626	0·5000
O(20)	0·2869	0·1891	0·5000
O(21)	0·0634	0·2645	0·5000
O(22)	0·2089	0·3574	0·5000
O(23)	0·4168	0·4346	0·5000
O(24)	0·1718	0·1007	0·5000
O(25)	0·3403	0·2795	0·5000
O(26)	0·1701	0·4439	0·5000

The average standard deviations for the oxygen atoms are 0·06 Å. Temperature factors for all atoms were fixed at $B = 1·0$ Å^2. The occupancy factor (*p*) for each oxygen atom is unity.

cordance with this it was observed that in each triplet of reflexions, the pair arising from the monoclinic crystals are not equal in intensity, although they lie symmetrically about the central spot. The reflexions arising from the monoclinic crystals are also more diffuse than those from the orthorhombic phase, presumably due to smaller domain regions.

The unit-cell dimensions of the orthorhombic phase are as previously listed (see also Table 3) whilst the the corresponding monoclinic unit-cell vectors will have identical magnitudes. The β angle was determined by measuring the separation of the 903 and $\bar{9}03$ reflexions. Reflexions from the monoclinic phase can be recognized by their diffuseness and also by their occurrence in pairs. On this basis it was possible to identify the space group of the orthorhombic phase as either *Pbam* or *Pba*2 and the monoclinic phase as $P2_1$ or $P2_1/m$. The former two space groups are identical, in (001) projection, as the plane group of both is *pgg*.

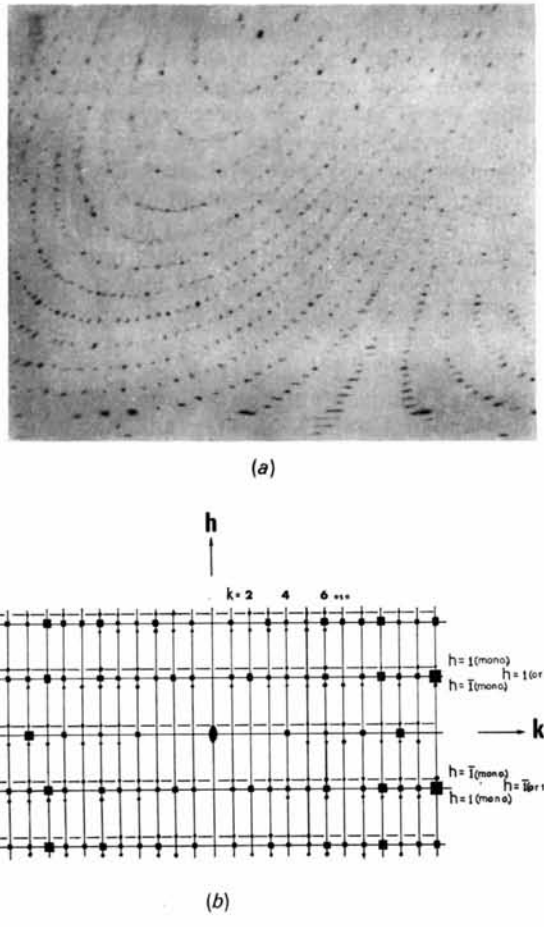

Fig. 4. (*a*) An *hk*2 equi-inclination Weissenberg photograph of the compound $Nb_{12}W_{11}O_{63}$. The spots split perpendicular to festoons having a constant *h* index and indicate an orthorhombic crystal intergrowing with a monoclinic crystal which is twinned on the (100) plane. (*b*) The *hk*2 weighted reciprocal lattice level constructed from the Weissenberg photograph in (*a*). The twin axis is perpendicular to this net.

Structure determination of the orthorhombic phase

Clearly it is impossible to separate sets of three-dimensional data for the two crystal systems and this unfortunate overlap is responsible for the troubles encountered in previous attempts at structure refinement. Separation of spots on the second Weissenberg level is reasonable if each spot is viewed through a microscope eyepiece. If the space group of the orthorhombic phase is *Pbam*, all atoms lie exactly in the (001) and (002) planes and the intensities of the *hk*0 and *hk*2 data will be very similar indeed. It is worthwhile noting that these sets of data will *not* be exactly the same since, although the geometric part of the structure factor expression will be identical for both levels, the relative scattering powers of the atoms will differ. However, if one assumes the *Z* coordinates of the appropriate atoms to be either zero or $\frac{1}{2}$, then it should be possible to refine the remaining positional parameters using *hk*2 data.

The *hk*2 intensity data for the orthorhombic phase were measured in the manner previously indicated, but with the use of a microscope eyepiece. The data were processed as before and twenty-eight of the octahedrally coordinated metal atoms were placed in positions 4(*g*) of space group *Pbam* and with the coordinates previously found for them. The remaining two six-coordinated metal atoms were placed in special positions 2(*c*). The location of the oxygen and seven-coordinated metal atoms was facilitated by the use of generalized electron density projections involving the *hk*2 data. The data were phased on the above metal atom contributions to the structure factors, for which purpose it was assumed that (Nb + W)/2 represented the average metal atom population at any one site.

The host lattice appeared to be essentially the same as that previously obtained from the combined *hk*0 data from the two intergrowth phases. However, the structure differs in that only eight of the twelve pentagonal rings are occupied (see Fig. 3). The statistical distribution of niobium and tungsten atoms over all octahedral metal sites is in accordance with the equal peak heights observed at these locations (62e). However, the pentagonal rings are occupied each to the same extent by atoms significantly lower in electron density content, thought to be niobium (48e) or half-tungsten atoms (42e). It was felt that a fuller knowledge

Table 3. *Crystallographic constants for the two intergrowth phases in the compound* $Nb_{12}W_{11}O_{63}$

Symmetry	Possible space group	Unit-cell dimensions			
		a	*b*	*c*	β
Orthorhombic	*Pbam*, *Pba*2	12·195 Å	36·740 Å	3·951 Å	
Monoclinic	$P2_1/m$, $P2_1$	12·195	36·740	3·951	90° 30′

of the composition of this orthogonal phase was needed before rigorous refinement procedures were adopted.

The composition of the orthorhombic phase

The complex of corner-sharing octahedra which constitutes the orthorhombic unit cell involves 30 metal atom sites and 90 oxygen atom sites. There is no reason to believe that these locations are anything but fully occupied by atoms. In addition there are 12 pentagonal rings each of which can accommodate one metal and one oxygen atom. The number of metal atoms in a unit cell is therefore $30+\Delta M$, where $0 \le \Delta M \le 12$, and the number of oxygen atoms is $90+\Delta O$ where $0 \le \Delta O \le 12$.

Suppose four pentagonal rings are completely filled with metal and oxygen atoms so that the compound $xNb_2O_5.yWO_3$ is stoichiometric.

Therefore, $2x+y=34$ and $5x+3y=94$. These simultaneous equations then give $x=8$ and $y=18$, corresponding to $8Nb_2O_5.18WO_3$ or the 4:9 compound. Thus, the compound $4Nb_2O_5.9WO_3$, if it had a unit-cell structure based upon three tetragonal-bronze unit cells, would have four pentagonal rings completely filled with metal and oxygen atoms. This has been shown to be the case by Sleight (1966).

Other solutions, for integral values of ΔM and ΔO between 0 and 12, are shown in Fig. 5, where the rectangular coordinates are the compositional variates x and y. All solutions lie within a parallelogram whose dimensions are governed by the limiting values of ΔM and ΔO. The 4:9 compositional line therefore passes through the point $\Delta M=4$, $\Delta O=4$, and no other points within the parallelogram lie on this line. This singular solution, corresponding to a whole number of atoms in the unit cell, represents a *stoichiometric* compound with no composition range. Other portions of the 4:9 line within the parallelogram correspond to fractional numbers of oxygen and metal atoms in the pentagonal rings, which are *non-stoichiometric* compounds.

It can be seen that the 6:11 compositional line does *not* pass through any one of these points. Instead, there are two points $\Delta M=4$, $\Delta O=3$ and $\Delta M=5$, $\Delta O=6$, which lie close to this line and correspond to compounds $9Nb_2O_5.16WO_3$ and $9Nb_2O_5.17WO_3$. These compounds are identified with the orthorhombic and monoclinic phase respectively; four metal atoms in pentagonal rings is not inconsistent with orthorhombic symmetry, and five metal atoms similarly placed may well conform with monoclinic symmetry. The average composition of these two phases, if they occur in equal proportions, is $6Nb_2O_5.11WO_3$.

The eight pentagonal rings which appear occupied in the orthorhombic unit cell are therefore each occupied with a half-tungsten atom and three-eighths of an oxygen atom. This composition arises since there are only four metal atoms and three oxygen atoms distributed over the eight rings. Peak heights had previously suggested that the metal atom in such a ring could either be a half-tungsten atom or a full niobium atom. If these atoms were niobium then ΔM would equal 8 rather than 4. This apparently unusual occupancy can be very easily explained and will be done so in the discussion of the structure.

Structure refinement

Now that the composition of the orthorhombic phase is known, $9Nb_2O_5.16WO_3$, and the nature of the occupancy of the pentagonal rings is understood, each remaining metal position must be occupied by the average atom (3Nb+2W)/5. The full-matrix least-squares program of Busing, Martin & Levy (1962) was used to refine the x, y and isotropic thermal parameters of the metal atoms and an overall scale factor. The function minimized was $\Sigma w(|F_{obs}|-|F_{calc}|)^2$. Frac-

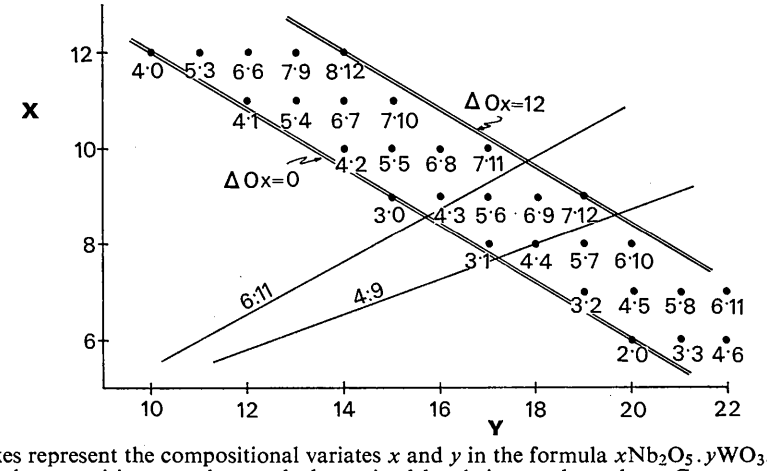

Fig. 5. The orthogonal axes represent the compositional variates x and y in the formula $xNb_2O_5.yWO_3$. Compounds of different compositions therefore have positions on the graph determined by their x and y values. Compounds with structures based upon three tetragonal-bronze unit cells lie within a parallelogram, two sides of which are shown. The full circles represent positions where integral numbers of metal atoms and oxygen atoms occupy pentagonal rings. The first number in each pair corresponds to the number of metal atoms in the pentagonal rings and the second number to the oxygen atoms in the same rings.

tional shifts were used (one-third) and initially, all observations were given unit weight. After several cycles the weighting scheme was adjusted so that w, for observed reflexions, was equal to $100/(F_{obs})^2$. The contributions from all the oxygen atoms whose z coordinates are zero were included in the calculated structure factors, but their atomic coordinates were not included as variates in the least-squares cycles. Instead, they were refined by difference Fourier series, which also indicated the positions of the oxygen atoms whose z coordinates are $\frac{1}{2}$. Refinement by difference Fourier series was found to be more effective for light atoms than least-squares methods, since a greater control can be maintained over the parameter shifts. Finally, a series of least-squares cycles was run in which all atoms contributed to the calculated structure-factors. The second weighting scheme was used and the two positional parameters, isotropic temperature factor and occupancy factor for each metal atom were allowed to vary. The final results, together with standard deviations, are listed in Table 4.

Negative temperature parameters result for all metal atoms (B was kept at unity for the light atoms). These may be due to the omission of absorption corrections to the observed data, the use of form factors for atoms in zero oxidation state, or to the singular use of $hk2$ data. Atomic peak shapes in generalized electron density projections with upper level data are sharper than the corresponding peaks observed in projection with the use of zero level data. The same effect is obtained by flattening the atomic form factors, *i.e.* by applying a negative temperature factor. The occupancy factors for the metal atoms do not significantly deviate from unity and therefore confirm the statistical distribution

Table 4. *Atomic parameters for* $9Nb_2O_5.16WO_3$

Standard deviations are given in brackets and refer to the last two (or three) places of the preceding number.

	Metal atoms*				
	x/a	y/b	z/c	p	B
M(1)	0·50000	0·00000	0·00000	1·122 (88)	4·12 (1·51) Å^2
M(2)	0·21003 (67)	0·02944 (24)	0·00000	1·013 (74)	−2·42 (30)
M(3)	0·42046 (74)	0·09944 (26)	0·00000	0·966 (70)	−2·19 (33)
M(4)	0·01177 (64)	0·16223 (23)	0·00000	0·882 (64)	−3·14 (30)
M(5)	0·29537 (101)	0·18972 (34)	0·00000	0·884 (73)	−1·57 (39)
M(6)	0·07001 (73)	0·26219 (26)	0·00000	0·866 (68)	−2·77 (33)
M(7)	0·20840 (66)	0·35570 (24)	0·00000	0·930 (66)	−2·75 (30)
M(8)	0·42515 (73)	0·43347 (29)	0·00000	0·847 (70)	−2·69 (31)
M(9)	0·33174 (109)	0·27593 (45)	0·00000	0·959 (79)	−1·92 (44)
M(10)	0·16775 (104)	0·44415 (36)	0·00000	1·076 (88)	−1·59 (46)
	M atoms 1–8 are (3Nb+2W)/5 M atoms 9 and 10 are W/2				
	Oxygen atoms				
O(1)	0·5122	0·0460	0·0000		
O(2)	0·0820	0·0430	0·0000		
O(3)	0·2720	0·0730	0·0000		
O(4)	0·3820	0·1425	0·0000		
O(5)	0·1700	0·1635	0·0000		
O(6)	0·1980	0·2410	0·0000		
O(7)	0·0100	0·2130	0·0000		
O(8)	0·1610	0·3114	0·0000		
O(9)	0·1020	0·3945	0·0000		
O(10)	0·2980	0·4010	0·0000		
O(11)	0·3280	0·0070	0·0000		
O(12)	0·3320	0·4660	0·0000		
O(13)	0·3660	0·3310	0·0000		
O(14)	0·3900	0·2290	0·0000		
O(15)	0·0120	0·1110	0·0000		
O(16)	0·5000	0·0000	0·5000		
O(17)	0·2027	0·0287	0·5000		
O(18)	0·4117	0·1008	0·5000		
O(19)	0·0117	0·1592	0·5000		
O(20)	0·2876	0·1888	0·5000		
O(21)	0·0840	0·2583	0·5000		
O(22)	0·2063	0·3579	0·5000		
O(23)	0·4167	0·4292	0·5000		
O(24)	0·3317	0·2759	0·5000		
O(25)	0·1678	0·4442	0·5000		

O(1) to O(23) are normal oxygen atoms. O(24) and O(25) are 3/8 oxygen atoms. Temperature factors were fixed at $B=1·0$ Å^2 and occupancy factors remained at unity.

of Nb and W atoms over octahedral metal sites and the occurrence of W/2 atoms in each of the eight pentagonal rings.

The data are seriously affected by extinction and double reflexion. The 0150 reflexion, a systematic absence, is quite intense on *hk*0 Weissenberg films [$30 \times F_{obs}$(min)]. This reflexion does not, however, appear on 0*kl* precession photographs. The *hk*2 data from the orthorhombic phase are also considerably overlapped by the *hk*2 data from the monoclinic phase. Nevertheless, the reliability index for all observed *hk*2 data is 0·19. The main contributing factor to this apparently high value is undoubtedly the deviation of the atomic *z* parameters from 0 and $\frac{1}{2}$. The tetragonal bronze is a polar structure and atoms are significantly displaced from the (001) and (002) planes (~0·1 Å). It is most probable that $9Nb_2O_5.16WO_3$ is also a polar structure with space group *Pba*2, and that atomic *z* parameters deviate significantly from 0 and $\frac{1}{2}$.

Attempts were made to grow single crystals of the individual compounds $9Nb_2O_5.16WO_3$ and $9Nb_2O_5.17WO_3$ so that exact details concerning the third positional parameter of each atom could be obtained. High purity niobium pentoxide and tungsten anhydride were intimately mixed in the correct proportions (±0·1 mg in 3-g batches) and heated in sealed platinum tubes at 1355°C for 68 hours before quenching. Good quality crystals were obtained, but these proved to contain the 4:9 and 3:8 phases. It is apparent that a much longer heat treatment is necessary to achieve equilibrium. In the meantime, the structure is sufficiently well defined to warrant description.

Description of the structure

The structure, as seen in (001) projection, is depicted in Fig. 3. There are eight crystallographically distinct octahedra of oxygen atoms, each centred about an average metal atom of composition (3Nb+2W)/5. The complex of corner-sharing octahedra which are generated from this fundamental set by the symmetry elements of the plane group *pgg* extends in a third direction parallel to (001), again by corner-sharing. Eight of the twelve pentagonal ring sites are each filled with (4W+3O)/8 atoms.

Table 5. *Ideal atomic coordinates for a* 3×1 *subcell unit derived from the tetragonal bronze structure*

Metal atoms

	x/a	*y/b*	*z/c*
M(1)	0·5000	0·0000	0·0183
M(2)	0·2159	0·0249	0·0438
M(3)	0·4252	0·0947	0·0438
M(4)	0·0000	0·1667	0·0438
M(5)	0·2841	0·1916	0·0438
M(6)	0·0748	0·2380	0·0438
M(7)	0·2159	0·3583	0·0438
M(8)	0·4252	0·4280	0·0438
M(9)	0·3279	0·2760	0·0161
M(10)	0·1721	0·4426	0·0161

Table 5 (*cont.*)

Oxygen atoms

	x/a	*y/b*	*z/c*
O(1)	0·507	0·052	0·0000
O(2)	0·066	0·049	0·0000
O(3)	0·279	0·074	0·000
O(4)	0·354	0·145	0·000
O(5)	0·155	0·164	0·000
O(6)	0·221	0·240	0·000
O(7)	0·993	0·218	0·000
O(8)	0·146	0·311	0·000
O(9)	0·066	0·382	0·000
O(10)	0·279	0·407	0·000
O(11)	0·155	0·497	0·000
O(12)	0·354	0·478	0·000
O(13)	0·345	0·331	0·000
O(14)	0·434	0·215	0·000
O(15)	0·007	0·115	0·000
O(16)	0·500	0·000	0·500
O(17)	0·216	0·025	0·500
O(18)	0·425	0·095	0·500
O(19)	0·000	0·167	0·500
O(20)	0·284	0·192	0·500
O(21)	0·075	0·238	0·500
O(22)	0·216	0·358	0·500
O(23)	0·425	0·428	0·500
O(24)	0·328	0·276	0·500
O(25)	0·172	0·443	0·500

Selected interatomic distances and angles have been calculated between atoms lying in the (001) plane. These are listed in Table 6 and must be used with caution since it has been assumed that all these atoms are coplanar. This is certainly not the actual case and the interatomic distances represent projected or minimum distances. Nevertheless they satisfactorily depict the packing situation. The metal atoms are displaced from

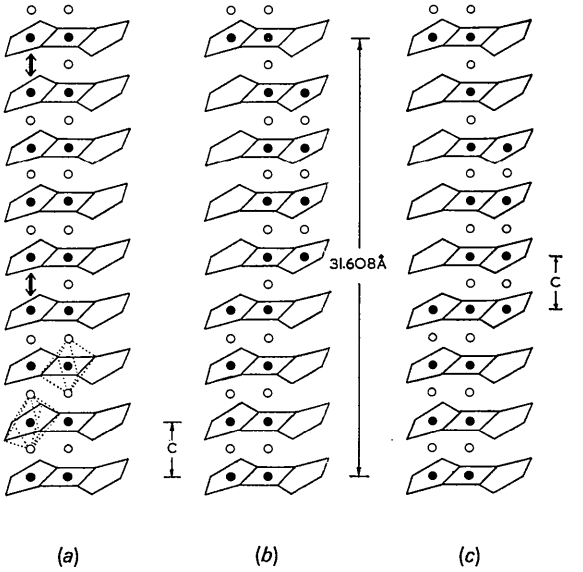

Fig. 6. A side view of a pentagonal tunnel running parallel, along the **c** direction, to strings of octahedra. (*a*) An electrostatically unfavourable way of arranging the tunnel-filling units. (*b*) The most probable arrangement of tunnel-filling units. (*c*) An alternative way of filling the pentagonal tunnels.

the centres of gravity of their surrounding octahedra of oxygen atoms and these displacements appear to be smallest for atoms M(1) and M(4), *i.e.* those atoms which have a negligible displacement in the original tetragonal-bronze structure. The remaining octahedra are considerably distorted, particularly those surrounding each *empty* pentagonal tunnel. The metal atoms are displaced towards the tunnel resulting in an appreciable distortion of the tunnel from a regular pentagonal shape. The O(13)1–O(14)1–O(15)1 angle of

Table 6. *Selected interatomic distances* (Å) *and angles* (°) *in the compound* $9Nb_2O_5.16WO_3$

The atomic numbering used is the same as in Table 4; the superscripts denote the following symmetry transformations of the parameters of Table 4:

[no superscript]	$x,\ y,\ z$
i	$\frac{1}{2}+x,\ \frac{1}{2}-y,\ \bar{z}$
ii	$\frac{1}{2}-x,\ \frac{1}{2}-y,\ \bar{z}$
iii	$\frac{1}{2}-x,\ \frac{1}{2}+y,\ \bar{z}$
iv	$\frac{1}{2}-x,\ -\frac{1}{2}+y,\ \bar{z}$
v	$\bar{1}-x,\ \bar{y},\ z$

M(1) octahedron		M(3) octahedron	
M(1) –O(11)	1·70	M(3) –O(11)	2·26
–O(21)	2·11	–O(13)	2·05
O(21)–O(11)	2·66	–O(14)	1·65
–O(11^{v})	2·76	–O(19^{i})	2·23
M(2) octahedron		O(11)–O(19^{i})	2·45
M(2) –O(12)	1·64	–O(13)	3·09
–O(13)	1·77	O(14)–O(19^{i})	3·01
–O(21)	1·66	–O(13)	2·88
–O(22^{iv})	2·38		
O(12)–O(22^{iv})	3·02		
–O(13)	2·56		
O(21)–O(22^{iv})	2·46		
–O(13)	2·52		
M(4) octahedron		M(6) octahedron	
M(4) —O(15)	1·93	M(6) –O(16)	1·74
–O(17)	1·87	–O(17)	1·95
–O(23^{ii})	1·79	–O(18)	2·12
–O(25)	1·88	–O(24^{ii})	2·22
O(15)—O(25)	2·73	O(17)–O(16)	2·51
–O(17)	2·67	–O(24^{ii})	2·58
O(23^{ii})–O(17)	2·39	O(18)–O(16)	2·63
–O(25)	2·78	–O(24^{ii})	3·62
M(5) octahedron		M(7) octahedron	
M(5) –O(14)	2·03	M(7) –O(18)	1·73
–O(15)	1·81	–O(19)	1·93
–O(16)	2·23	O(20)	1·99
–O(24)	1·85	–O(23)	2·13
O(14)–O(24)	3·18	O(18)–O(19)	3·13
–O(15)	2·70	–O(23)	2·60
O(16)–O(24)	2·38	O(20)–O(19)	2·40
–O(15)	2·87	–O(23)	2·70
M(8) octahedron			
M(8)—O(12^{i})	2·10		
–O(20)	1·96		
–O(22)	1·65		
–O(25^{i})	1·95		
O(12^{i})–O(22)	3·07		
–O(25^{i})	2·64		
O(20) –O(22)	2·42		
–O(25^{i})	2·65		
M(9) pentagonal bipyramid			
M(9)—O(16)	2·10	O(17^{i})–O(23) –O(18)	121·3
–O(20)	1·96	O(23) –O(18) –O(16)	96·1
–O(22)	1·65	O(18) –O(16) –O(24)	110·6
–O(25^{i})	1·95	O(16) –O(24) –O(17^{i})	113·8
O(17^{i})–O(24)	2·58	O(24) –O(17^{i})–O(23)	98·2
–O(23)	2·39		
O(18) –O(23)	2·60		
–O(16)	2·63		
O(16) –O(24)	2·38		

Table 6 (*cont.*)

M(10) pentagonal bipyramid			
M(10)—O(11^{ii})	1·93	O(19)—O(20)—O(22)	105·6
–O(19)	1·99	O(20)—O(22)—O(21^{iii})	117·8
–O(20)	2·24	O(22)—O(21^{iii})–O(11^{ii})	97·4
–O(21^{iii})	2·31	O(21^{iii})–O(11^{ii}) –O(19)	108·4
–O(22)	2·16	O(11^{ii}) –O(19)—O(20)	110·9
O(19)—O(11^{ii})	2·45		
–O(20)	2·40		
O(22)—O(20)	2·42		
–O(21^{iii})	2·47		
O(21^{iii})–O(11^{ii})	2·76		
Empty pentagonal bipyramid			
O(12)–O(13)	2·56	O(12)–O(13)–O(14)	143·2
–O(25)	2·64	O(13)–O(14)–O(15)	78·9
O(14)–O(13)	2·88	O(14)–O(15)–O(25)	118·4
–O(15)	2·70	O(15)–O(25)–O(12)	116·2
O(15)–O(25)	2·73	O(25)–O(12)–O(13)	83·4

The estimated standard deviations of metal–oxygen distances are 0·07 Å, for oxygen–oxygen 0·10 Å and for the angles, 5°.

78·9° very significantly differs from the normal value of 108°. On the other hand the occupied pentagonal tunnels, *i.e.* those containing atoms M(9) and M(10) are much more regular and *smaller* than the empty tunnels. Ideal atomic coordinates for a 3×1 subcell unit derived from the tetragonal bronze structure are given in Table 5 for comparison with the actual values observed in the compound $9Nb_2O_5.16WO_3$.

The rather unusual occupancy of the filled pentagonal rings may be interpreted in the following way.

Fig. 6(*a*) illustrates a side view of a pentagonal tunnel running parallel, along the **c** direction, to a string of octahedra. Within this tunnel the regular sequence of W–O–W–O *etc.* is interrupted after 4 tungsten atoms since, for every four tungsten atoms, there are only 3 oxygen atoms in the pentagonal tunnels. Continuing to fill this same tunnel would result in two positive tungsten ions adjacent and not separated by a negative oxygen anion thus – W–O–W–O–W–O–W↔W–O *etc.* [Fig. 6(*a*)]. Rather than countenance this electrostatically unfavourable situation the *adjacent* tunnel commences to fill [Fig. 6(*b*)] until, once more, a W–W interaction is encountered. The original tunnel then reverts to filling, so that in any one tunnel there is a 'filling-unit' of atoms, *i.e.* W–O–W–O–W–O–W followed by four metal and five oxygen vacancies. The periodicity along any one tunnel is therefore $8c=31{\cdot}608$ Å. The adjacent tunnel-filling unit may be positioned according to Fig. 6(*b*), which is electrostatically the most favourable, or according to Fig. 6(*c*) where a displacement of the tunnel filling-unit by 3·951 Å occurs. This situation may be likened to a stacking fault and the filling-units in adjacent pentagonal tunnels may be displaced from the symmetrical arrangement in Fig. 6(*b*) by an integral number of *c* units.

This picture of the pentagonal tunnel-filling process in the compound $9Nb_2O_5.16WO_3$, where the stoichiometry and unit-cell dimensions determine that four metal atoms and three oxygen atoms shall occupy the pentagonal bipyramidal positions, explains in a simple manner why

(1) eight pentagonal tunnels are occupied
(2) these eight tunnels occur in pairs, the components of which are separated by a filled string of corner-sharing octahedra (see Fig. 3)
(3) each tunnel is half-filled.

Order, disorder and intergrowth

The host structure of corner-sharing octahedra obviously is completely ordered. The disorder occurs in the filling of the pentagonal tunnels. In any one pentagonal tunnel running parallel to the *c* axis, there is a sequence of atoms W–O–W–O–W–O–W, which constitutes a filling-unit, followed by four metal and five oxygen vacancies. The periodicity along this tunnel is 31·608 Å. All occupied pentagonal tunnels are the same in this respect but there is no rule dictating how the tunnel-filling-units will pack with respect to one another in adjacent or, for that matter, any neighbouring tunnel. A randomness in the filling of pentagonal tunnels appears to destroy the 31·608 Å periodicity in any one tunnel and the overall or average periodicity in the **c** direction is 3·951 Å, as observed.

The coexistence and intergrowth of structures at the unit-cell level is not an uncommon occurrence. Fleet, Chandrasekhar & Megaw (1966) have shown that in the plagioclase feldspar, bytownite, there are translation-related locations of the same structure within the one crystal, giving rise to small anti-phase domains whose origins are related by the vector $\frac{1}{2}(\mathbf{a}+\mathbf{b}+\mathbf{c})$. Andersson, Mumme & Wadsley (1966) have shown that intergrowth, at the unit-cell level, of equal proportions of the adjoining phases, $WNb_{12}O_{33}$ and $W_3Nb_{14}O_{44}$, leads to a phase of composition $W_4Nb_{26}O_{77}$. In fact, they propose that ranges of homogeneity and composition range within a solid solution may arise from *ordered* phases which intergrow in varying proportions and at the unit cell level.

It is now proposed to examine the possibility that complete ordering occurs in the compound $9Nb_2O_5.16WO_3$ and that the apparent disorder, or fractional occupancy of certain atomic positions, arises

from the intergrowth of differently oriented domains in which the atoms are completely ordered. The preparation of a stable phase in the binary system $Nb_2O_5.WO_3$ involves heat treatment and annealing of the specimen for as long as 1000 hours. Under these conditions it might be expected that the atoms would order into fixed positions rather than distribute themselves at random over a number of atomic sites. This was found to be the case with the compound $NaMo_6O_{17}$ (Stephenson, 1966). At first sight the 17 oxygen atoms appeared to be randomly distributed over the 18 sites of a trigonally distorted perovskite structure. However, the true structure proved to be monoclinic and consistent with the *ordered* distribution of 34 oxygen atoms in the unit cell.

Electrostatically the most favoured manner of stacking filling-units in adjacent tunnels, *i.e.* those separated by a string of octahedra, is shown in Fig. 6(*b*). If this type of ordering occurs for *every* pair of tunnels, then a unit cell results, which is shown in Fig. 7(*a*). This is a 'domain' unit cell representative of the structural unit in a single-crystal domain where no randomness occurs but where the filling of one pentagonal tunnel influences the manner in which an adjacent pentagonal tunnel positions its filling-unit. The domain unit cell has dimensions $a=12{\cdot}195$, $b=36{\cdot}740$, $c=31{\cdot}608$ Å, space group $Pnb2_1$, and therefore differs from experimentally observed unit cells in c axial length and space group. Because of this conflicting experimental evidence one would tend to discount the occurrence of complete ordering of tunnel filling-units, and favour the random filling of these pentagonal tunnels, *i.e.* randomness in the z coordinates of the tunnel filling-units. However, it is still possible that ordered domains do exist in the composite crystal provided that these domains do not extend very far along the **c** direction (although they must not be so small as to produce diffuse streaks on the X-ray diagrams), and that these domains are oriented in the same manner as those in the coexisting monoclinic phase, *i.e.* twinned on the (100) plane. A diagrammatic representation of this situation is shown in Fig. 7. The host structure exhibits a twofold axis parallel to **c** and the rotation by 180° of the domain unit cell shown in Fig. 7(*a*) produces a domain cell [Fig. 7(*b*)] which has an identical host lattice, but in which the tunnel filling-units are displaced along the c axis by 31·608/2 Å. The operation is therefore not strictly twinning. It is equivalent to introducing a stacking fault in the filling of the pentagonal tunnels, thereby destroying the 31·608 Å periodicity of the whole structure along the **c** direction and also the twofold screw axis. The matrix of intergrowing domains is depicted in Fig. 7(*c*). The description of the structure as a stacking together of layers, or domains, in which there is a maximum degree of order within the layers, but where stacking faults occur along the c-axis direction, classifies the structure as an OD (order–disorder) arrangement (Dornberger-Schiff, 1956, 1965).

The monoclinic phase and intergrowth

The corresponding unit-cell translational vectors for the phases $9Nb_2O_5.16WO_3$ and $9Nb_2O_5.17WO_3$ are identical (Table 3), which means that the host structure of corner-sharing octahedra, based upon the tetragonal bronze structure and described above for the orthorhombic phase, extends continuously through both orthorhombic and monoclinic phases coexisting in the one crystal of average composition $6Nb_2O_5.11WO_3$.

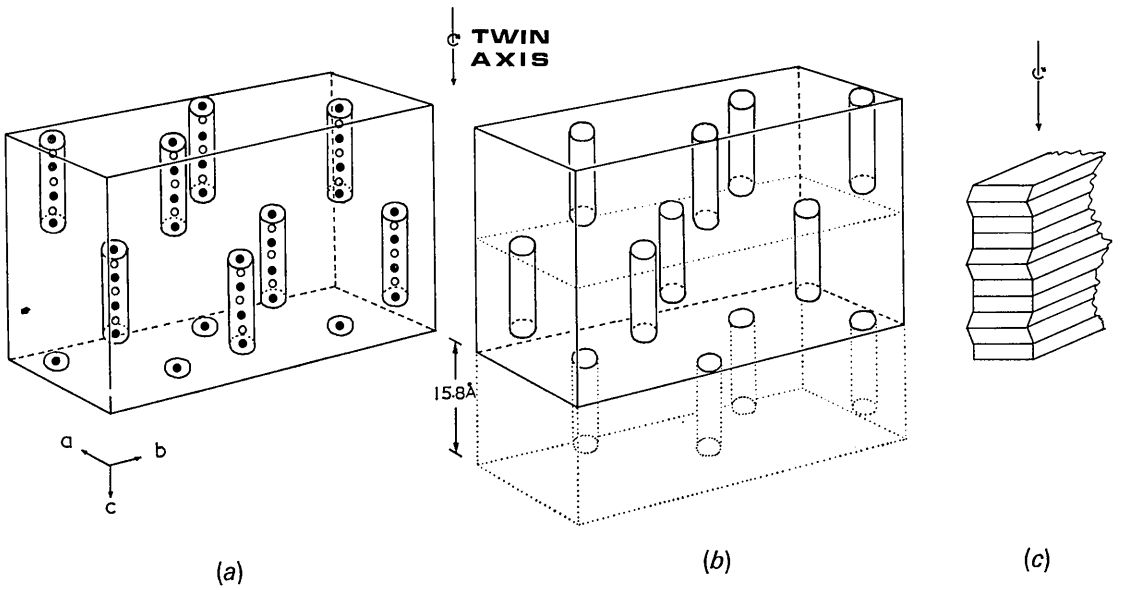

Fig. 7. (*a*) A 'domain' unit cell containing tunnel-filling units (shown as cylinders) arranged according to (*b*). (*b*) A 'domain' unit cell related to the cell in (*a*) by a twin axis parallel to [001]. (*c*) 'Domain' cells of the orthorhombic and monoclinic phases intergrowing in a twinned crystal.

The x and y coordinates for similar atoms of this host structure will be the same for both phases, resulting in complete intergrowth. The different symmetries of the two phases arise as a result of different pentagonal tunnels being occupied.

The space group of the monoclinic phase must be $P2_1$ (see Table 3) since there are obviously no mirror planes perpendicular to the screw axes shown in Fig. 8. Actually the distribution of atoms of the host structure of the monoclinic phase is consistent with the space group $P2_1/a$ but nevertheless, $h0l$ data are observed with $h=2n+1$. The glide plane is therefore destroyed by the manner in which the pentagonal tunnels are filled and the number of equaivalent positions becomes 2 rather than 4.

The $\Delta M:\Delta O$ ratio for the monoclinic phase is 5:6 (Fig. 5) and therefore the situation probably arises which is found in the orthorhombic phase: adjacent tunnels will be alternatively filled owing in this case, to anion–anion repulsion as compared with cation–cation repulsion in the $9Nb_2O_5.16WO_3$ compound. Although further discussion of the monoclinic phase is bound to be speculative, its inclusion in the present paper is felt to be justified on the grounds that it emphasizes those aspects of the problem that deserve further study.

A suitable tunnel filling-unit can be assumed to be O–W–O–W–O–W–O, and the periodicity along such a half-filled pentagonal tunnel will be 31·608 Å. An untwinned *domain* cell in which these pentagonal tunnels are ordered in a favourable electrostatic manner, *i.e.* according to Fig. 7(*a*), has a unit cell with dimensions $a=12{\cdot}195$, $b=33{\cdot}740$, $c=31{\cdot}608$ Å, $\beta=90°30'$. The postulated structure for the monoclinic cell is shown in projection in Fig. 8. The half-filled pentagonal tunnels (full circles) correspond in position to similar tunnels in the orthorhombic unit cell so as to permit intergrowth of the domains of monoclinic and orthorhombic phases (see below). The stoichiometry $9Nb_2O_5.17WO_3$ requires that two remaining pentagonal tunnels per unit cell be completely filled with tungsten and oxygen atoms, and these tunnels are shown as hatched circles in Fig. 8. There appears to be a choice between these two tunnels, so selected, and the remaining empty set. However, the two different unit cells which result are related as twins and the relationship is according to the twin law found for the monoclinic phase, *i.e.* the twin axis is parallel to **c** and the twin plane is (100).

Further discussion of the monoclinic phase must await verification of the proposed structure, but nevertheless, the manner in which domains of the monoclinic phase intergrow with domains of orthorhombic phase is apparent and is illustrated in Fig. 9. The eight partially occupied pentagonal tunnels of Fig. 7 are drawn into a straight line and viewed sideways. Each tunnel is separated from its neighbour by a string of corner-sharing octahedra which extends continuously through both monoclinic and orthorhombic phases, forming an overall host structure. The two phases intergrow so that the filling-units of adjoining tunnels

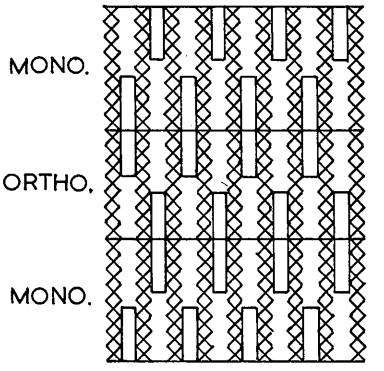

Fig. 9. A diagrammatic representation of the intergrowth of monoclinic and orthorhombic domains. Infinite strings of corner-sharing octahedra extend through both structures. The pentagonal tunnel-filling units are shown as rectangles.

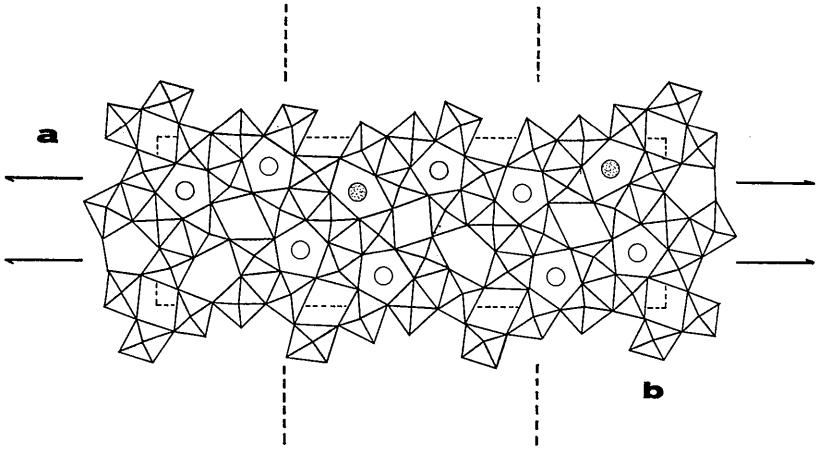

Fig. 8. Symmetry elements of the host structure of the compound $9Nb_2O_5.17WO_3$. The circles represent metal and oxygen atoms (superposed), which occupy pentagonal rings in the proposed structure of the monoclinic phase. Projection along [001].

of each phase can combine to give a large filling-unit for each tunnel, in the following way:

NEW UNIT

O–W–O–W–O–W–O—|—W–O–W–O–W–O–W

monoclinic unit | orthorhombic unit

INTERFACE

The metal-deficient monoclinic tunnel-filling unit readily interfaces with the oxygen-deficient orthorhombic tunnel-filling unit to give much larger units in which the metal to oxygen ratio is 1:1.

Building principles

The structures of the stable phases in the region $Nb_2O_5.WO_3$–WO_3 are based upon a tetragonal-bronze subcell. As the pentagonal tunnels are filled, in keeping with the stoichiometry of the substance, the host-structure becomes distorted, its symmetry elements (*P4bm*) degenerate and the unit cell becomes larger,

Table 7. *A summary of the subcell units, plane groups and space groups for the compounds examined in this study*

Composition Nb_2O_5 : WO_3	Size of subcell	Plane group of *c*-axis projection	Space group
host	1×1	*p4g*	*P4bm*
4 9	3×3	*pgg*	$P2_12_12$
9 16	1×3	*pgg*	*Pba*2
9 17	1×3	*pg*	$P2_1$
2 7	2×2	*p*4	—

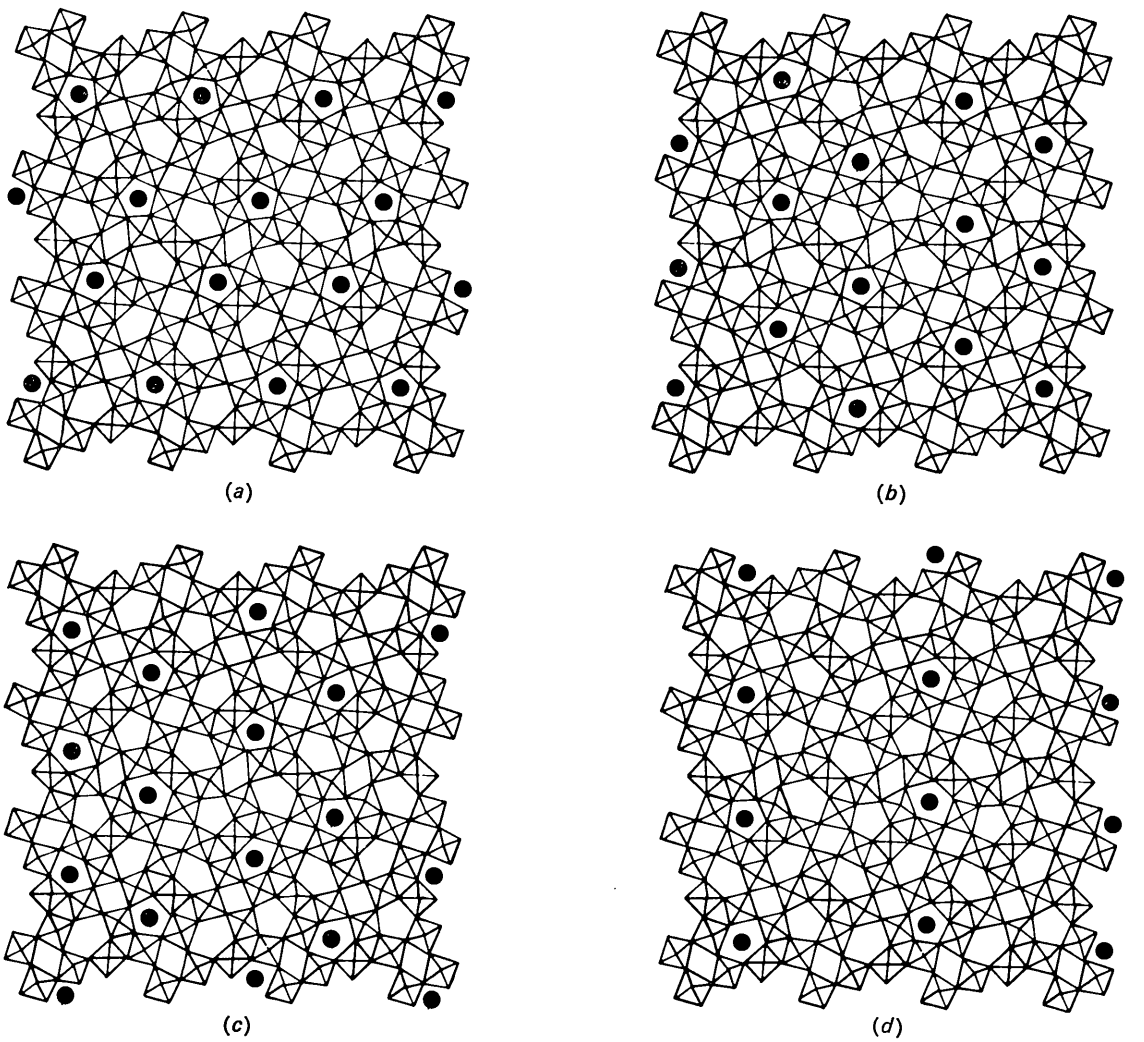

Fig. 10. (*a*) The structure of $4Nb_2O_5.9WO_3$. The fully filled pentagonal tunnels (large, full circles) are packed in hexagonal array. (*b*) The structure of $9Nb_2O_5.16WO_3$. The large filled circles represent filled pentagonal tunnels in the lower half of a 'domain' cell. There is hexagonal packing. (*c*) A projection of the top half of a 'domain' unit cell of the compound $9Nb_2O_5.16WO_3$. The packing of pentagonal tunnels is hexagonal. (*d*) The packing of the completely filled pentagonal tunnels in the compound $9Nb_2O_5.17WO_3$ is approximately cubic.

in multiples of the basic tetragonal cell. Table 7 summarizes the space groups and numbers of subcells associated with unit cells of the compounds so far examined. The plane groups of projections of these structures, viewed down the *c* axis, are also given. (These can be very useful, as will be shown in the derivation of the structure of $2Nb_2O_5.7WO_3$.)

The compound $4Nb_2O_5.9WO_3$ has been listed with a unit cell based upon 9 tetragonal subcell units. In his X-ray examination of this substance, Sleight (1966) found only 3 subcell units (Table 1) but noted that the crystals exhibited a strong tendency to twin about the [130] axis and therefore give the superficial appearance of being tetragonal with a $\simeq$36 Å. His crystals were obtained from a Nb_2O_5:WO_3 mixture in the ratio 1:3. We have examined single crystals grown from a 4:9 mix, in which there is no twinning. The unit cell is orthorhombic with $a=36{\cdot}69$, $b=36{\cdot}57$ and $c=3{\cdot}945$ Å, thus containing 9 tetragonal subcell units. The structure is essentially the same as that derived by Sleight and will be described in a later communication.

The filled pentagonal tunnels are stacked in a close-packed array parallel to **c**. The arrangement in the compound $4Nb_2O_5.9WO_3$ is close-packed hexagonal [Fig. 10(*a*)]; each filled tunnel is surrounded by six other filled tunnels at distances of 9·26–11·75 Å. A similar packing mode is found in the compound $9Nb_2O_5.16WO_3$. In the ordered *domain* unit cells those pentagonal tunnels which are marked [Fig. 10(*b*)] are completely filled at the one level of *c*, whilst the remaining partially occupied pentagonal tunnels are empty at this level, and *vice versa*. At any one level parallel to (001) the pentagonal tunnels are therefore filled in a close-packed hexagonal array, each tunnel being surrounded by six neighbours at distances between 9·04 and 11·77 Å [Fig. 10(*b*)].

The compound $9Nb_2O_5.17WO_3$ has a structure very similar to the previous compound and hexagonal close-packing is found at any one level along **c** for the partially occupied pentagonal tunnels. On the other hand, the completely filled pentagonal tunnels have a cubic packing arrangement (shown as filled tunnels in Fig. 10(*d*). If the average cell ($c=3{\cdot}951$ Å) is considered rather than the domain unit cell ($c=31{\cdot}608$ Å) the filled and partially filled pentagonal tunnels are stacked in close-packed hexagonal array.

The structure of $2Nb_2O_5.7WO_3$

The compound $2Nb_2O_5.7WO_3$ ($Nb_4W_7O_{31}$) forms between a minimum temperature of about 1245 °C and the probable congruent melting point of 1357 °C. The unit cell is tetragonal with dimensions $a=24{\cdot}264$, $c=3{\cdot}924$ Å. 'Single-crystal' photographs are extremely poor in that they contain data from multiple crystals, oriented so that their *c* axes are parallel. Nevertheless, the structure can be confidently predicted in the following manner, using the principles developed above.

Fig. 11 depicts the compositional parallelogram for a 2×2 matrix of tetragonal-bronze subcells. The 2:7 composition line passes through the point $\Delta M=4$, $\Delta O=4$, an indication that four of the pentagonal tunnels in the unit cell of $8Nb_2O_5.28WO_3$ are completely filled with metal and oxygen atoms.

The plane group of the host structure of corner-sharing octahedra, when viewed down the fourfold axis of the tetragonal cell, is *p*4 [Fig. 12(*a*)]. The four filled pentagonal tunnels are therefore related according to the four equivalent positions 4(*d*) of plane group *p*4 (no. 10). There are also four possible sets of these filled tunnels generated from either *A*, *B*, *C* or *D* [Fig. 12(*a*)]. The structures so derived from sites *A* and *B* are the same in that they involve filled pentagonal tunnels grouped together in fours [Fig. 12(*b*)]. The structures derived from sites *C* and *D* are more electrostatically favourable and are to be preferred since they involve a *cubic close-packing* of filled pentagonal tunnels [Fig. 12(*b*)]. Twenty per cent of these tunnels in the overall cubic close-packed array are vacant.

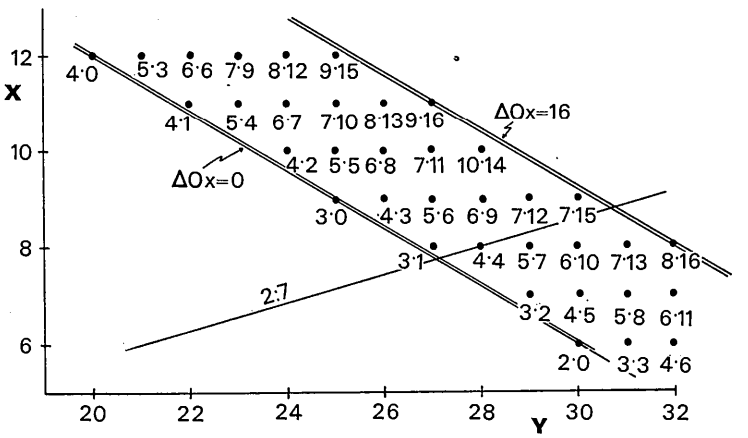

Fig. 11. A graphical representation of the relationship between composition and the number of pentagonal tunnels filled with metal and oxygen atoms. The graph is calculated for a structure based upon 4 tetragonal-bronze subcells.

Table 8. *Ideal atomic parameters derived for the compound* $2Nb_2O_5.7WO_3$

Atom	*x/a*	*y/b*	*z/c*
M(1)	0·2500	0·0000	0·0183
M(2)	0·2500	0·5000	0·0438
M(3)	0·1079	0·0374	0·0438
M(4)	0·3922	0·4627	0·0438
M(5)	0·1421	0·2874	0·0438
M(6)	0·3580	0·2126	0·0438
M(7)	0·0374	0·3571	0·0438
M(8)	0·4626	0·1080	0·0438
M(9)	0·2874	0·3580	0·0438
M(10)	0·2126	0·1421	0·0438
M(11)	0·1640	0·4140	0·0161
O(1)	0·390	0·140	0·000
O(2)	0·111	0·361	0·000
O(3)	0·361	0·340	0·000

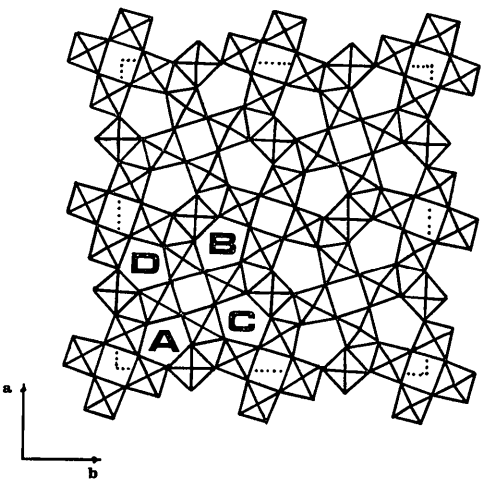

(*a*)

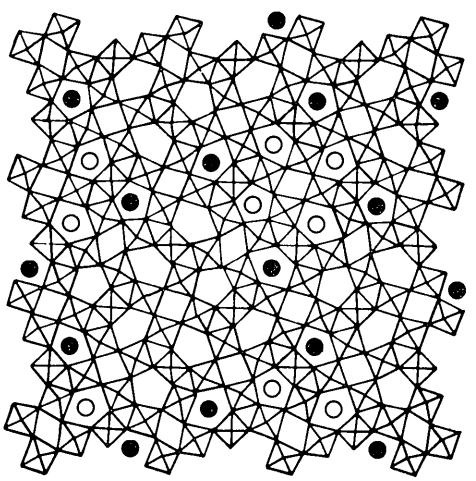

(*b*)

Fig. 12. (*a*) A projection down the [001] axis of the tetragonal host structure of the compound $2Nb_2O_5.7WO_3$. (*b*) The open circles represent the structure derived for the compound $2Nb_2O_5.7WO_3$ by filling pentagonal tunnels of the type marked A in (*a*). The filled circles represent the proposed structure for this compound. The completely filled pentagonal tunnels are packed in cubic array.

Table 8 (*cont.*)

Atom	*x/a*	*y/b*	*z/c*
O(4)	0·140	0·111	0·000
O(5)	0·004	0·173	0·000
O(6)	0·497	0·328	0·000
O(7)	0·247	0·423	0·000
O(8)	0·254	0·078	0·000
O(9)	0·173	0·497	0·000
O(10)	0·328	0·004	0·000
O(11)	0·423	0·254	0·000
O(12)	0·078	0·247	0·000
O(13)	0·033	0·073	0·000
O(14)	0·467	0·427	0·000
O(15)	0·217	0·323	0·000
O(16)	0·283	0·177	0·000
O(17)	0·073	0·467	0·000
O(18)	0·427	0·033	0·000
O(19)	0·323	0·283	0·000
O(20)	0·177	0·217	0·000
O(21)	0·250	0·000	0·500
O(22)	0·250	0·500	0·500
O(23)	0·108	0·037	0·500
O(24)	0·392	0·463	0·500
O(25)	0·142	0·287	0·500
O(26)	0·358	0·213	0·500
O(27)	0·037	0·357	0·500
O(28)	0·463	0·108	0·500
O(29)	0·287	0·358	0·500
O(30)	0·213	0·142	0·500
O(31)	0·164	0·414	0·500

The atomic coordinates, derived for an idealized structure based upon the tetragonal-bronze structure, are listed in Table 8.

The author would like to acknowledge the encouragement of Dr A.D.Wadsley and Dr R.S.Roth. He is also indebted to the Australian Institute of Nuclear Science and Engineering for a research grant.

References

ANDERSSON, S. (1965). *Acta Chem. Scand.* **19**, 2285.
ANDERSSON, S. & LUNDBERG, M. (1966). Private communication.
ANDERSSON, S., MUMME, W. G. & WADSLEY, A. D. (1966). *Acta Cryst.* **21**, 802.
BUSING, W. R., MARTIN, K. O. & LEVY, H. A. (1962). *ORFLS, a Fortran Crystallographic Least-Squares Program*, U.S. Atomic Energy Commission Report ORNL-TM-305.
DAUBEN, C. H. & TEMPLETON, D. H. (1955). *Acta Cryst.* **8**, 841.
DORNBERGER-SCHIFF, K. (1956). *Acta Cryst.* **9**, 593.
DORNBERGER-SCHIFF, K. & DUNITZ, J. D. (1965). *Acta Cryst.* **19**, 471.
FIEGEL, L. J., MOHANTY, G. P. & HEALY, J. H. (1964). *J. Chem. and Eng. Data*, **9**, 365.
FLEET, S. G., CHANDRASEKHAR, S. & MEGAW, H. D. (1966). *Acta Cryst.* **21**, 782.
GATEHOUSE, B. M. & WADSLEY, A. D. (1964). *Acta Cryst.* **17**, 1545.
GOLDSCHMIDT, H. J. (1960). *Metallurgia*, **62**, 373.
GRAHAM, J. & WADSLEY, A. D. (1961). *Acta Cryst.* **14**, 379.
HÄGG, G. & MAGNÉLI, A. (1954). *Rev. Pure Appl. Chem.* **4**, 235.

Table 9. *A list of absolute values of observed and calculated structure factors*

The columns read, from left to right, *hkl*|*F*(obs.)| and |0·01 *F*(calc.)|. Unobserved reflexions have been given *F*(obs.) values of zero.

0	4	2	0.5399	0.9876	3	17	2	0.7500	0.5541	6	17	2	1.9599	2.0526	9	25	2	4.6699	5.0075
0	6	2	0.2299	0.1288	3	18	2	6.5699	7.7255	6	18	2	4.3799	4.4625	9	26	2	0.0000	2.5402
0	8	2	0.4599	0.8292	3	19	2	3.9399	3.5067	6	19	2	0.0000	2.1859	9	27	2	7.5799	8.7538
0	10	2	5.4099	3.6361	3	20	2	0.0000	1.4157	6	20	2	0.0000	0.7968	9	28	2	2.2699	0.7834
0	12	2	3.5999	2.3291	3	21	2	1.8399	2.0117	6	21	2	1.3799	1.0002	9	29	2	2.5099	1.6962
0	14	2	1.3999	0.5522	3	22	2	0.0000	1.1430	6	22	2	0.0000	0.8935	9	30	2	4.6699	4.5117
0	16	2	2.9099	1.9405	3	23	2	3.2500	2.6343	6	23	2	1.4499	2.3823	9	31	2	2.0699	1.9308
0	18	2	0.7199	0.8411	3	24	2	6.7500	7.0784	6	24	2	5.1399	4.1507	9	32	2	3.6899	1.3631
0	20	2	1.7399	2.1454	3	25	2	2.0099	0.2857	6	25	2	0.0000	1.4550	9	33	2	3.3599	3.4495
0	22	2	1.1399	0.4603	3	26	2	0.0000	0.0325	6	26	2	0.0000	1.5321	9	34	2	0.0000	0.2053
0	24	2	7.6899	7.8690	3	27	2	0.0000	1.9026	6	27	2	2.9899	2.9000	9	35	2	0.0000	0.8761
0	26	2	0.0000	1.0394	3	28	2	3.2699	2.2248	6	28	2	4.9799	4.7110	9	36	2	0.0000	2.9661
0	28	2	0.0000	0.3380	3	29	2	2.2899	2.7515	6	29	2	0.0000	1.0072	10	0	2	7.1599	7.2384
0	30	2	7.5799	7.1834	3	30	2	1.2500	1.3244	6	30	2	5.0899	5.2188	10	1	2	2.9699	2.6866
0	32	2	4.8999	4.7381	3	31	2	1.7999	1.1009	6	31	2	1.8199	0.9454	10	2	2	0.0000	0.4501
0	34	2	0.0000	0.3862	3	32	2	2.0299	1.4701	6	32	2	3.2500	1.6814	10	3	2	5.5699	5.5536
0	36	2	2.5699	2.5648	3	33	2	2.7399	1.7003	6	33	2	6.8099	6.4713	10	4	2	2.9799	2.8376
0	38	2	0.0000	1.6452	4	0	2	3.8999	2.3413	6	34	2	3.0000	2.8054	10	5	2	1.7299	1.7925
1	1	2	0.2899	0.4795	4	1	2	1.7699	0.9948	6	35	2	3.0399	2.0249	10	6	2	5.1399	5.7620
1	2	2	0.5199	0.9351	4	2	2	0.0000	0.1755	6	36	2	9.6399	11.1405	10	7	2	0.0000	1.0885
1	3	2	0.2799	0.9546	4	3	2	8.0099	9.5751	6	37	2	3.3099	2.8521	10	8	2	0.0000	0.1365
1	4	2	0.2599	0.1282	4	4	2	1.3799	0.6365	6	38	2	1.8199	0.9060	10	9	2	0.0000	0.5075
1	5	2	0.4599	0.8226	4	5	2	1.1299	0.6930	6	39	2	2.7899	2.6937	10	10	2	0.0000	0.5853
1	6	2	1.0799	1.4625	4	6	2	5.3699	6.4488	7	1	2	0.0000	0.4475	10	11	2	2.1899	0.6861
1	7	2	0.0000	0.0229	4	7	2	1.4799	1.5878	7	2	2	1.0299	0.7316	10	12	2	0.0000	0.5516
1	8	2	1.1799	0.9770	4	8	2	1.0499	0.4547	7	3	2	7.5899	10.4798	10	13	2	2.2099	0.8642
1	9	2	7.9899	5.5096	4	9	2	1.4299	1.2164	7	4	2	1.7599	1.8681	10	14	2	2.5599	1.3601
1	10	2	1.6999	0.2518	4	10	2	1.4399	0.9734	7	5	2	0.0000	0.2987	10	15	2	6.2399	6.0336
1	11	2	2.0399	1.1007	4	11	2	1.8899	0.5570	7	6	2	0.0000	0.6638	10	16	2	2.7399	3.5884
1	12	2	8.8199	9.6283	4	12	2	1.2099	1.1598	7	7	2	1.4099	1.7897	10	17	2	3.0299	3.8690
1	13	2	1.9099	1.2953	4	13	2	3.2500	2.1417	7	8	2	2.2899	2.3616	10	18	2	4.6599	4.2090
1	14	2	0.9399	0.5029	4	14	2	0.0000	0.0341	7	9	2	2.5899	2.5445	10	19	2	3.0199	1.4475
1	15	2	0.9599	0.3245	4	15	2	2.1399	2.3369	7	10	2	3.2099	2.1695	10	20	2	2.2199	1.6961
1	16	2	1.0899	0.2626	4	16	2	1.7299	1.8965	7	11	2	0.0000	0.8900	10	21	2	2.2099	0.6761
1	17	2	2.1699	1.2249	4	17	2	0.0000	0.2556	7	12	2	2.6799	2.8017	10	22	2	2.6799	1.6771
1	18	2	1.2500	0.9998	4	18	2	1.5499	2.0081	7	13	2	3.3799	3.4306	10	23	2	0.0000	1.4789
1	19	2	0.8999	0.9461	4	19	2	2.1399	1.6769	7	14	2	0.0000	0.6073	10	24	2	3.2599	2.3299
1	20	2	2.1799	2.1224	4	20	2	1.0999	0.1565	7	15	2	5.0699	4.7925	10	25	2	2.9599	4.0285
1	21	2	8.6999	9.9354	4	21	2	2.8499	3.3039	7	16	2	0.0000	1.0257	10	26	2	2.3599	1.8089
1	22	2	3.2399	3.0540	4	22	2	2.4499	2.1627	7	17	2	0.0000	0.3101	10	27	2	6.5000	6.8241
1	23	2	1.5399	0.7385	4	23	2	0.0000	0.8480	7	18	2	0.0000	0.8248	10	28	2	1.9299	2.1900
1	24	2	3.2899	3.3175	4	24	2	2.3099	2.3245	7	19	2	0.0000	1.3433	10	29	2	0.0000	2.1552
1	25	2	1.7399	1.6165	4	25	2	1.7799	1.3635	7	20	2	2.1999	0.7120	10	30	2	1.9199	2.2697
1	26	2	0.0000	0.0363	4	26	2	2.4699	2.6639	7	21	2	6.9599	8.0960	11	1	2	0.0000	0.6948
1	27	2	1.9099	1.5530	4	27	2	10.0198	10.0617	7	22	2	3.3499	2.3212	11	2	2	3.2699	2.9736
1	28	2	2.1399	1.1305	4	28	2	0.0000	0.1657	7	23	2	0.0000	1.6849	11	3	2	3.2699	3.4635
1	29	2	2.3699	1.7721	4	29	2	3.0699	1.0637	7	24	2	4.7199	4.3617	11	4	2	0.0000	0.0031
1	30	2	4.2199	3.6452	4	30	2	0.0000	0.2498	7	25	2	2.0199	1.3977	11	5	2	2.3999	1.5192
1	31	2	4.9899	5.2984	4	31	2	2.5699	0.6445	7	26	2	1.8199	2.1868	11	6	2	9.2299	10.3102
1	32	2	2.1999	2.6780	4	32	2	0.0000	1.2264	7	27	2	2.4199	1.8111	11	7	2	1.8199	0.7828
1	33	2	2.3999	2.2447	4	33	2	0.9999	0.9136	7	28	2	2.5799	0.6161	11	8	2	1.2899	0.9499
1	34	2	2.5799	2.7196	4	34	2	2.5699	0.4404	7	29	2	0.0000	1.5777	11	9	2	3.1599	2.9187
1	35	2	0.0000	0.4912	4	35	2	2.6899	3.8131	7	30	2	0.0000	0.0470	11	10	2	0.0000	0.1796
1	36	2	4.7999	4.5847	4	36	2	4.2999	4.2872	7	31	2	2.3499	2.6895	11	11	2	2.2399	1.5600
1	37	2	0.8899	0.4353	4	37	2	3.6299	3.3952	7	32	2	0.0000	1.6265	11	12	2	2.4199	2.2239
1	38	2	1.9599	1.3589	4	38	2	2.7399	2.0288	7	33	2	5.1099	5.0157	11	13	2	4.6699	4.2185
1	39	2	3.9799	3.7950	4	39	2	4.2699	4.7637	7	34	2	2.4699	2.0696	11	14	2	0.0000	1.4662
2	0	2	0.0000	0.5322	5	0	2	0.0000	0.0000	7	35	2	4.2799	5.0088	11	15	2	2.3999	1.3897
2	1	2	0.4599	0.5153	5	1	2	0.0000	0.2031	7	36	2	3.2199	2.6910	11	16	2	3.0999	4.0771
2	2	2	0.0000	0.2966	5	2	2	2.1299	1.9853	7	37	2	2.1599	2.3687	11	17	2	0.0000	0.5452
2	3	2	0.9199	1.2410	5	3	2	0.0000	0.0390	8	0	2	5.7599	7.2948	11	18	2	7.2699	7.6382
2	4	2	0.4599	0.8485	5	4	2	0.0000	0.2700	8	1	2	0.0000	0.6600	11	19	2	0.0000	0.4749
2	5	2	0.2500	0.4366	5	5	2	0.0000	0.1546	8	2	2	0.0000	0.0619	11	20	2	0.0000	1.1790
2	6	2	2.1399	2.5922	5	6	2	1.4599	1.2730	8	3	2	3.1299	3.2583	11	21	2	4.4299	4.0223
2	7	2	2.9199	1.8502	5	7	2	0.6899	0.0787	8	4	2	2.4299	2.1096	11	22	2	2.2099	1.6017
2	8	2	2.4099	1.4258	5	8	2	0.6999	0.1979	8	5	2	0.9599	0.7985	11	23	2	2.4499	0.4106
2	9	2	7.2199	6.2225	5	9	2	4.2699	3.9842	8	6	2	5.2999	5.4175	11	24	2	9.2299	8.7535
2	10	2	1.1199	0.6394	5	10	2	0.0000	0.3175	8	7	2	2.0999	0.6757	11	25	2	2.0499	2.3776
2	11	2	2.6799	1.9295	5	11	2	1.1499	0.5490	8	8	2	1.4199	0.3313	11	26	2	1.8299	2.0373
2	12	2	5.8199	5.8882	5	12	2	2.6699	3.0455	8	9	2	7.7699	7.9476	11	27	2	2.6899	1.9338
2	13	2	0.0000	0.3165	5	13	2	0.0000	0.1272	8	10	2	0.0000	1.0200	12	0	2	3.2799	3.8048
2	14	2	0.0000	0.0462	5	14	2	0.0000	0.2034	8	11	2	2.8099	2.3797	12	1	2	0.0000	0.2979
2	15	2	1.3799	1.1118	5	15	2	10.1298	12.4213	8	12	2	2.1699	1.4514	12	2	2	0.0000	0.5411
2	16	2	0.0000	0.3448	5	16	2	2.9899	1.9960	8	13	2	0.0000	0.5416	12	3	2	4.9699	4.5894
2	17	2	1.6799	0.5822	5	17	2	2.1699	1.7768	8	14	2	0.0000	0.5145	12	4	2	2.2199	0.3645
2	18	2	4.1099	6.7236	5	18	2	4.7799	3.9960	8	15	2	3.8099	4.4772	12	5	2	2.7199	2.8119
2	19	2	1.8599	2.3935	5	19	2	0.0000	0.5350	8	16	2	2.0299	2.1450	12	6	2	7.2299	8.2520
2	20	2	1.5099	1.4904	5	20	2	2.1099	1.7974	8	17	2	0.0000	0.7897	12	7	2	3.3699	2.6259
2	21	2	0.7899	0.3324	5	21	2	4.5199	4.4557	8	18	2	4.3699	3.2742	12	8	2	2.0099	1.7444
2	22	2	3.3499	3.2430	5	22	2	2.4099	1.5803	8	19	2	3.0099	2.5186	12	9	2	2.5299	2.2282
2	23	2	1.7299	2.0984	5	23	2	0.0000	0.2878	8	20	2	0.0000	0.5228	12	10	2	0.0000	0.2529
2	24	2	5.6799	4.9855	5	24	2	3.1499	3.6065	8	21	2	5.5699	5.7039	12	11	2	2.3499	2.6035
2	25	2	3.0099	1.5080	5	25	2	3.6499	3.5397	8	22	2	2.3799	2.0781	12	12	2	4.6599	5.0233
2	26	2	1.0799	0.8656	5	26	2	2.9699	1.0668	8	23	2	2.7199	1.1790	12	13	2	1.7500	0.4695
2	27	2	2.3899	1.5418	5	27	2	6.0699	5.4312	8	24	2	8.6599	8.7791	12	14	2	0.0000	0.9173
2	28	2	3.2999	3.1726	5	28	2	0.0000	1.3420	8	25	2	4.9199	5.4209	12	15	2	2.7099	1.8156
2	29	2	0.0000	0.0590	5	29	2	2.2099	2.3617	8	26	2	0.0000	0.5307	12	16	2	0.8499	0.8521
2	30	2	4.4399	5.4069	5	30	2	5.6099	5.9677	8	27	2	3.3899	1.9808	12	17	2	1.4399	3.0118
2	31	2	0.0000	1.1897	5	31	2	5.6299	5.5348	8	28	2	2.1999	2.9244	12	18	2	11.2198	12.7696
2	32	2	2.5499	1.0720	5	32	2	0.0000	2.4177	8	29	2	3.1899	4.0260	12	19	2	3.3999	2.9924
2	33	2	7.7999	9.0293	5	33	2	0.0000	0.3355	8	30	2	3.9799	2.7632	12	20	2	0.0000	1.0158
2	34	2	5.4799	4.9717	5	34	2	4.1899	3.0079	8	31	2	0.0000	0.0982	12	21	2	3.7399	3.5841
2	35	2	2.2299	1.2523	5	35	2	2.4799	2.3244	8	32	2	2.4699	1.0530	13	0	2	0.0000	0.0000
2	36	2	7.3899	7.2170	5	36	2	2.9599	2.0236	8	33	2	8.1899	8.2709	13	1	2	0.0000	0.9357
2	37	2	0.0000	0.2574	5	37	2	6.5000	5.4973	8	34	2	4.4499	4.8937	13	2	2	0.0000	2.6739
2	38	2	1.7299	2.6506	5	38	2	0.0000	0.9455	8	35	2	2.4099	2.9104	13	3	2	3.0799	2.4341
2	39	2	6.7199	7.2221	5	39	2	5.6399	6.0250	9	1	2	1.3399	1.5420	13	4	2	4.1699	4.0400
3	0	2	0.6899	0.0000	6	0	2	0.0000	0.3691	9	2	2	1.3399	1.1706	13	5	2	3.6999	1.9182
3	1	2	2.2699	1.4657	6	1	2	2.1999	2.1529	9	3	2	1.5499	2.3169	13	6	2	7.2099	8.1270
3	2	2	1.2999	0.7702	6	2	2	1.1299	0.9006	9	4	2	1.7500	1.3271	13	7	2	0.0000	0.7819
3	3	2	6.7500	5.7007	6	3	2	1.0199	0.9497	9	5	2	1.3599	0.2610	13	8	2	1.8599	1.6769
3	4	2	1.7099	1.1016	6	4	2	1.7699	1.0612	9	6	2	1.7699	1.1291	13	9	2	6.3499	6.4930
3	5	2	2.4499	1.4025	6	5	2	1.1499	0.3393	9	7	2	0.0000	0.4076	13	10	2	3.4699	2.9329
3	6	2	7.4199	6.9088	6	6	2	3.5099	6.6168	9	8	2	1.8099	1.6812	13	11	2	1.6199	0.2967
3	7	2	1.5799	1.0201	6	7	2	1.0799	0.9733	9	9	2	0.0000	2.1408	13	12	2	6.1399	6.0028
3	8	2	0.6499	0.2533	6	8	2	1.5399	1.5304	9	10	2	1.8499	1.3761	13	13	2	1.9299	2.2500
3	9	2	5.9099	6.2896	6	9	2	6.4299	8.1538	9	11	2	0.0000	0.1328	13	14	2	4.1699	4.8246
3	10	2	0.0000	0.1985	6	10	2	1.5099	1.6549	9	12	2	9.7799	10.1918	13	15	2	5.0899	5.9899
3	11	2	1.0499	0.8937	6	11	2	1.5399	1.4482	9	13	2	1.7099	1.4487	13	16	2	0.0000	0.3643
3	12	2	1.4299	0.9476	6	12	2	0.7699	1.2374	9	14	2	1.5000	1.4704	13	17	2	0.0000	0.3670
3	13	2	0.4799	0.3657	6	13	2	1.0000	0.7517	9	15	2	7.3199	6.2050	14	0	2	10.8798	13.9612
3	14	2	1.5499	1.1113	6	14	2	2.5799	2.0351	9	16	2	0.0000	0.6521	14	1	2	0.0000	0.1515
3	15	2	4.0899	3.8504	6	15	2	4.7699	4.1263	9	17	2	2.1899	1.0790	14	2	2	0.0000	0.1048
3	16	2	0.0000	0.4379	6	16	2	2.0999	1.6812	9	18	2	3.2399	3.4054	14	3	2	1.8299	1.3544
										9	19	2	2.7199	1.1209	14	4	2	2.0999	1.2662
										9	20	2	2.2299	3.1693	14	5	2	2.7599	3.3927
										9	21	2	2.7399	2.3136	14	6	2	0.0000	0.3446
										9	22	2	1.2899	1.1874	14	7	2	5.5599	5.4548
										9	23	2	3.4099	1.7845	14	8	2	0.0000	0.9156
										9	24	2	3.6299	2.9239	14	9	2	2.1199	2.0877

HOERNI, J. A. & IBERS, J. A. (1954). *Acta Cryst.* **7**, 744.
KIHLBORG, L. (1963). *Acta Chem. Scand.* **17**, 1485.
KOVBA, L. M. & TRUNOV, V. K. (1962). *Dokl. Akad. Nauk SSSR*, **147**, 622.
MAGNÉLI, A. (1949). *Ark. Kemi*, **1**, 213.
ROTH, R. S. & WADSLEY, A. D. (1965). *Acta Cryst.* **19**, 26.
ROTH, R. S. & WARING, J. L. (1966). *J. Res. Nat. Bur. Stands.* **70A**, 281.
SIME, J. (1961). In *Computing Methods and the Phase Problem in X-ray Crystal Analysis*. Eds. Pepinsky, Robertson and Speakman, London: Pergamon Press.
SLEIGHT, A. (1966). *Acta Chem. Scand.* **20**, 1102.
SLEIGHT, A. & MAGNÉLI, A. (1964). *Acta Chem. Scand.* **18**, 2007.
STEPHENSON, N. C. (1965). *Acta Cryst.* **18**, 496.
STEPHENSON, N. C. (1966). *Acta Cryst.* **20**, 59.
THOMAS, L. H. & UMEDA, K. (1957). *J. Chem. Phys.* **26**, 293.

Acta Cryst. (1968). B**24**, 653

The Structure of Cobalt Mercury Thiocyanate, $Co(NCS)_4Hg$

BY J. W. JEFFERY AND K. M. ROSE

*Department of Crystallography, Birkbeck College, London University, Malet Street, London, W.C.*1, *England*

(*Received* 15 *June* 1967)

Accurate intensity measurements using photometry of integrating Weissenberg photographs from a spherical crystal have enabled the structure of $Co(NCS)_4Hg$ to be solved in considerable detail. $a=11{\cdot}109$, $c=4{\cdot}379$. Space group $I\bar{4}$. $Z=2$. The structure was solved from three-dimensional Patterson and Fourier syntheses and refined by least squares; $R=4{\cdot}2\%$. The effects of secondary extinction and anomalous dispersion were investigated and C and N clearly distinguished in the presence of a considerable proportion of heavy atoms. The combination of two tetrahedrally coordinated atoms, Hg and Co, has produced a most unusual arrangement in which the Hg and Co atoms are held apart by four spirals, each containing 4 SCN bridges, which are interlinked so that any one SCN bridge takes part in eight spirals. Anomalous dispersion effects enable a distinction to be made between the *a* and *b* axes.

Introduction

The determination of the crystal structure of this compound (which is of importance in connexion with the investigation of paramagnetic anisotropy and polarized-light absorption spectra (Figgis & Nyholm, 1958; Ferguson, 1960; Cotton, Goodgame & Sacco, 1961; Figgis, Gerloch & Mason, 1964) and the spatial distribution of the mercury valency bonds in mercuric tetrathiocyanates) was first attempted (Jeffery, 1947) by two-dimensional Patterson and Fourier syntheses and by the use of a few critical general reflexions. The accuracy of the intensity measurements was insufficient to solve the structure completely and this provided the incentive for prolonged investigations of the factors involved in accuracy in intensity measurement (Jeffery, 1963; Rose & Jeffery, 1964; Jeffery & Rose, 1964; Jeffery & Whitaker, 1965). Cobalt mercury thiocyanate was used for part of these investigations and it was decided to complete the collection of accurate three-dimensional data and to find how much information it was possible to obtain about a structure in which the ratio of heavy to light atoms is greater than the ratio of carbon to hydrogen atoms in organic compounds, and where, in addition, there are large absorption effects. One of the objectives was to establish the exact sequence in the SCN bridge.

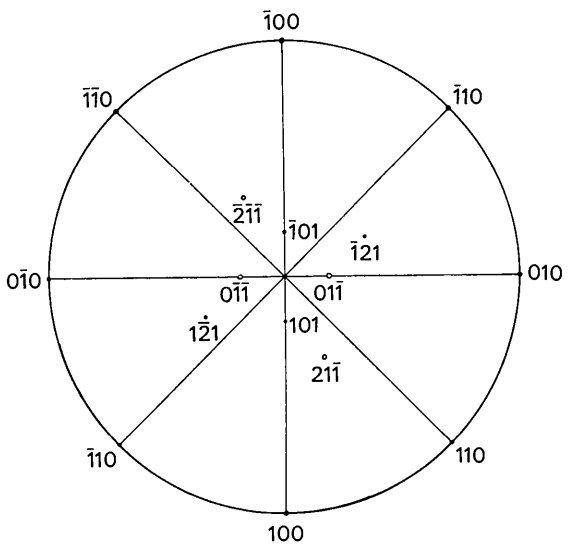

Fig. 1. Stereogram drawn from the optical goniometric measurements of a small double-ended crystal.

The primary crystallographic data have been given in the form suggested by Kennard, Speakman & Donnay (1967) unless stated otherwise.